Control of Voltage Source Inverter using Linear Quadratic Regulator for the three phase Grid integrated Renewable Energy System

R. Vinifa **A. Kavitha**
Department of Electrical and Electronics Engineering, College of Engineering, Guindy, Anna University, Chennai, India, Tel: 91-9442912448, Email :rvinifa@yahoo.com

Abstract*-Highly efficient power electronic converter promotes the integration of renewable energy sources (RES) to the grid with the evolution of control techniques in the field of power electronics. In this paper, the optimal Linear Quadratic Regulator (LQR) is implemented to govern the flow of real and reactive power from RES to the grid through current controlled voltage source inverter (CCVSI). The CCVSI behaves as shunt active power filter along with power conversion operation. The design of LQR is carried out using the proposed single phase equivalent circuit with lesser number of state variables. This shows the reduction of complexity by minimizing the number of weighing variables. To show the supremacy of LQR, the results are compared with conventional hysteresis controller in terms of Total Harmonic Distortion (THD) and power factor. To exemplify the potency of the controller, two modes of operation depends on the RES availability is implemented. The simulation and experimental results prove the performance of controllers.*

Keywords- *Current Controlled Voltage Source Inverter, Instantaneous p-q theory, Hysteresis Controller, Linear Quadratic Regulator.*

1. Introduction

Due to enormous increase in power demand, electrical power systems are getting overloaded [1,2]. This leads to the exponential increase in the usage of renewable energy sources (RES). By the advent of power electronic converters, RES is integrated with the electrical power system [3,4]. But the usage of power electronic devices and non-linear loads deteriorate the quality of power in the electrical system [5 - 7]. Therefore, an appropriate regulatory framework is to be followed for the distribution system to guarantee the reliable and efficient operation of the system.

In addition to the power converter, shunt active power filters [8 – 12] are used to mitigate the power quality issues. This increases the additional hardware cost. Hence, a current controlled voltage source inverter (CCVSI) is employed in this work for the twofold purpose of power conversion and power quality improvement [13]. The performance of CCVSI is based on the reference current generation [14]. The generated reference currents compensate the reactive and harmonic components. Various techniques are presented in literature [15 – 18] to generate reference currents. In this work, instantaneous p-q theory is used. It uses instantaneous quantities instead of average quantities. It eliminates the reactive power in transient states and harmonic currents [15]. A control technique is essential to track the reference currents.

In literature, many researchers proposed several control techniques to integrate the RES with the grid. The implementation of hysteresis controller is simple, but its variable switching frequency causes resonance and switching losses. Fixed switching frequency is obtained by comparing the output with the carrier wave in a conventional Proportional Integral (PI) controller with pulse width modulation (PWM). But steady state error is present in the output if sinusoidal reference is followed. The steady state error is eliminated by using proportional Resonant (PR) controller, but its performance depends on the controller which

operates in resonant frequency [2]. In terms of response profile, control effort requirement and robustness with respect to system nonlinearities, the optimal Linear Quadratic Regulator (LQR) is superior [19, 20]. Hence, LQR, the optimal pole placement controller is used in this work to track the sinusoidal references with fixed switching frequency, good stability margins and transient response. To prove the supremacy of LQR, the hysteresis controller is compared.

This paper is organized as follows: Section II explains the general description of RES integration with the grid and the control methodology. The generation of reference current using instantaneous p-q theory is presented in section III. Section IV details the single phase circuit, modeling, hysteresis controller and LQR design. Section V and VI give the simulation and experimental results respectively. This paper is concluded in section VII.

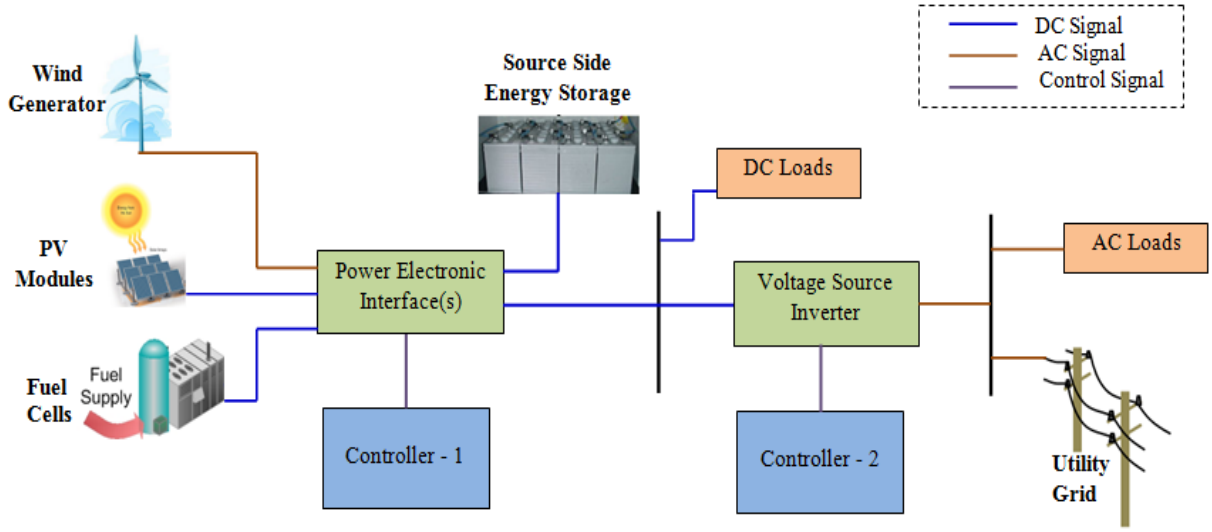

Fig. 1 General schematic of RES integrated with grid

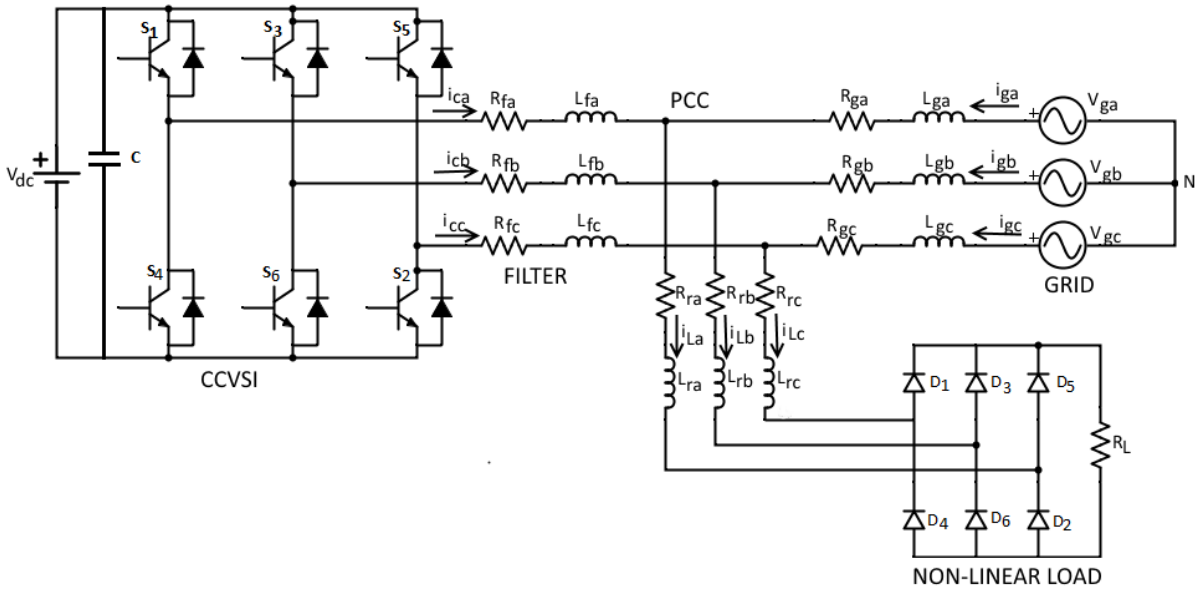

Fig. 2 Power Circuit Diagram of the grid connected inverter

2. System description

Different RESs are connected to the grid through power electronic converters, which is shown in fig. 1. The maximum power is derived from RES using power electronic interface which is controlled by controller -1. The extracted energy from RES is stored in the storage device, and it is delivered to the grid through CCVSI which is controlled by controller- 2. The controller-2 synchronizes and monitors the grid, reduces the harmonics at point of common coupling (PCC) and controls the real and reactive power flow between RES, grid and load.

Depending on the availability of RES power (P_{RES}), the modes of operation is divided into two. In the first mode of operation, P_{RES} is considered as lower than the load power (P_L). Hence the load is shared by the RES and grid. P_{RES} is taken as greater than load power in the second mode of operation. Here the excess power generated by the RES is supplied to the grid.

The dc link is modeled as dc source as shown in fig. 2 with the assumption of maximum power extracted from RES is stored in the battery. The amount of stored energy depends on the power availability in RES. Through CCVSI, filter inductors (L_{fa}, L_{fb}, L_{fc}) and its leakage resistances (R_{fa}, R_{fb}, R_{fc}), the dc source is connected to the grid. The grid inductances and its leakage resistances are represented as L_{ga}, L_{gb}, L_{gc} and R_{ga}, R_{gb}, R_{gc} respectively. The diode bridge rectifier feeding a resistance which is a non-linear load is connected to the PCC through rectifier link inductors (L_{ra}, L_{rb}, L_{rc}) and its corresponding leakage resistances (R_{ra}, R_{rb}, R_{rc}). The non-linear load draws harmonic and reactive power components from PCC which affects the quality of power in the grid. To improve the quality of power in the grid, the switches in the CCVSI are properly switched by a suitable controller in such a way that the inverter currents (i_{ca}, i_{cb}, i_{cc}) follow their corresponding reference currents (i_{ca}^*, i_{cb}^*, i_{cc}^*). Thus the reference currents are generated to maintain the grid currents (i_{ga}, i_{gb}, i_{gc}) sinusoidal with unity power factor. In this work, the reference currents are generated using instantaneous p-q theory and the controllers used are hysteresis and LQR.

3. Reference Current Generation Using Instantaneous P-Q Theory

The p-q theory is based on the instantaneous values instead of average values. It uses the αβ0 transformation known as Clarke transformation to obtain the reference currents. While generating reference currents the amount of real power flow from RES to the grid/load, reactive power compensation and harmonic reduction are taken into consideration.

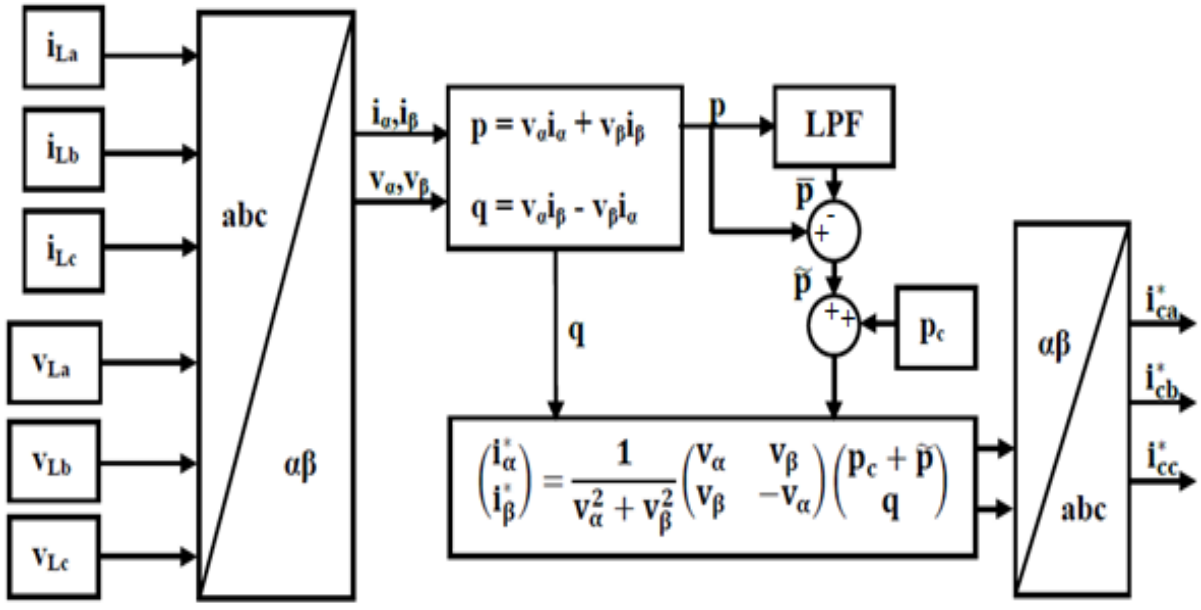

Fig. 3 Reference current generation using instantaneous p-q theory

The reference currents for the inverter ($i_{c\alpha}^*$, $i_{c\beta}^*$) in αβ coordinates are calculated as

$$\begin{bmatrix} i_{c\alpha}^* \\ i_{c\beta}^* \end{bmatrix} = \frac{1}{v_\alpha^2 + v_\beta^2} \begin{bmatrix} v_\alpha & v_\beta \\ v_\beta & -v_\alpha \end{bmatrix} \begin{bmatrix} p_c + \tilde{p} \\ q \end{bmatrix} \quad (1)$$

Where, p_c is the preferred real power demand from RES. $\tilde{p}$ is the oscillating component of the real power and q is the reactive power. The inverter reference currents in abc coordinates are calculated by transforming the αβ variables to abc variable by using inverse Clarke transformation. Fig. 3 shows the implementation of instantaneous p-q theory.

4. Design Of Controllers

To track the reference currents, the pulses are generated using hysteresis controller and LQR technique.

A. Hysteresis Controller (HC)

This is a simple and conventional technique to implement. It does not depend on load parameters. The main disadvantage is its variable switching frequency which leads to resonance problem and high switching losses. The implementation of hysteresis controller per phase is depicted in fig. 4. The error is calculated by finding the difference between the reference inverter current (i_c^*) and the actual inverter current. According to the error, the pulses are generated.

The control logic is

$$u = \begin{cases} -1, & i \geq i_c^* + h \\ 1, & i \leq i_c^* - h \end{cases} \quad (2)$$

Where, h is the width of the hysteresis band. The actual current is forced to follow the reference current by making the actual current to stay within the hysteresis band.

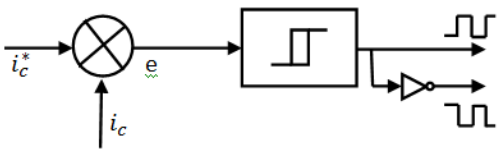

Fig. 4 Implementation of Hysteresis Controller per phase

B. Linear Quadratic Regulator (LQR)

To minimize the tracking error, an optimal control problem, LQR is used to determine the control strategies over a period of time. The drawback of variable switching frequency present in hysteresis controller is eradicated using LQR by comparing the error with the constant frequency triangular wave. Initially, the mathematical modeling is derived to determine the control law of LQR. To simplify the modeling, a simplified equivalent circuit shown in fig. 5 is developed for the three phase grid connected renewable energy system [21]. In the figure, $u.V_{dc}$ represents the CCVSI output voltage in which is the control variable for switching, R_f and L_f are the resistance and inductance of filter per phase, R_g and L_g are the resistance and inductance of grid per phase, R_L and L_L are the resistance and inductance of load per phase and v_g is the grid voltage.

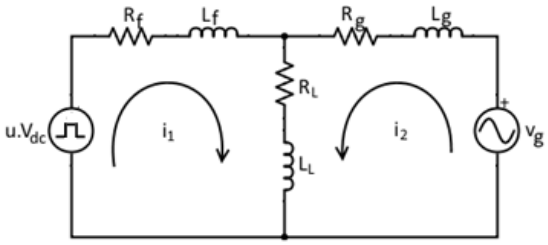

Fig. 5 Single Phase Equivalent Circuit of Grid Connected CCVSI.

Applying Kirchoff's voltage law, the differential equations of the circuit is written as

$$R_f i_1 + L_f \frac{di_1}{dt} + R_L(i_1 + i_2) + L_L \frac{d(i_1+i_2)}{dt} = uV_{dc}$$

$$R_g i_2 + L_g \frac{di_2}{dt} + R_L(i_1 + i_2) + L_L \frac{d(i_1+i_2)}{dt} = v_g \quad (3)$$

Taking loop currents i_1 and i_2 as state variables x_1 and x_2 respectively, the state equations are written as in (4),

$$\begin{pmatrix} \dot{x}_1 \\ \dot{x}_2 \end{pmatrix} = \begin{pmatrix} a_{11} & a_{12} \\ a_{21} & a_{22} \end{pmatrix} \begin{pmatrix} x_1 \\ x_2 \end{pmatrix} + \begin{pmatrix} b_{11} & b_{12} \\ b_{21} & b_{22} \end{pmatrix} \begin{pmatrix} v_g \\ u \end{pmatrix}$$

$$\text{i.e.)}\ \dot{X} = AX + BU \quad (4)$$

Where the coefficients of system matrix and input matrix are

$$a_{11} = \frac{-(R_f+R_L)L_g - R_f L_L}{(L_f+L_L)L_g + L_f L_L} \qquad a_{12} = \frac{-R_L L_g + R_g L_L}{(L_f+L_L)L_g + L_f L_L}$$

$$a_{21} = \frac{-R_L L_f + R_f L_L}{(L_f+L_L)L_g + L_f L_L} \qquad a_{22} = \frac{-(L_f+L_L)R_g - R_L L_f}{(L_f+L_L)L_g + L_f L_L}$$

$$b_{11} = \frac{-L_L}{(L_f+L_L)L_g + L_f L_L} \qquad b_{12} = \frac{V_{dc}L_g + V_{dc}L_L}{(L_f+L_L)L_g + L_f L_L}$$

$$b_{21} = \frac{L_f+L_L}{(L_f+L_L)L_g + L_f L_L} \qquad b_{22} = \frac{-V_{dc}L_L}{(L_f+L_L)L_g + L_f L_L} \quad (5)$$

In LQR technique, the error is minimized by deriving the optimal state feedback control law to place the poles in desired locations as

$$u = -K(X^* - X) \quad (6)$$

Where X is the actual state vector, X^* is the desired state vector and K is the feedback gain matrix. The value of K is found by solving the Algebraic Riccati Equation (ARE) of

$$A^T P + PA + Q - PBR^{-1}B^T P = 0 \quad (7)$$

and the solution is

$$K = R^{-1}B^T P \quad (8)$$

Here, Q is the positive semi-definite diagonal symmetry matrix which is formed by the weighing variables of X, R is the positive definite diagonal symmetry matrix which is formed by the weighing variables of U and P is the symmetry matrix which is found from ARE. The weights are properly chosen according to the task played in this control. In this work, the CCVSI current plays a major role, thus more weightage is given to CCVSI current.

In this work, the simplified equivalent circuit reduces the order of the state equations. Thus the number of weighing variables is reduced which minimizes the complexity design of LQR.

5. Simulation Results

By using the specifications shown in table 1, the system is simulated using MATLAB/SIMULINK environment to compare the efficacy of the controllers. A three phase diode bridge rectifier feeding a resistance draws non-sinusoidal current with real power of 290 W, reactive power of 84 var and THD of 24%. The CCVSI is controlled to achieve unity power factor and low total harmonic distortion in the grid side. If the power flows towards PCC from grid / inverter, the sign convention is taken as positive. Similarly, if the power flows from PCC to load, the sign convention is taken as positive.

Table 1
Parameters of the circuit

Parameters	Values
DC Link Voltage	300 V
Grid side Voltage (max. value)	100 V
CCVSI filter Inductance	50 mH
CCVSI filter Resistance	0.4 Ω
Feeder Inductance	0.01 mH
Feeder Resistance	1 ohm
Rectifier Link Inductance	40 μH
Rectifier Link Resistance	0.1 Ω
Rectifier DC side Resistance	50 Ω

To evaluate the performance of the controllers, the simulation is performed in two modes in the presence of non-linear load. The simulated waveforms of inverter, grid, load voltages and current in phase 'a' and its real and reactive power flow are shown in fig. 6. The load current, inverter current and grid current are operated with an amplification factor of 10, 10 and 20 respectively to increase the perceptibility.

Mode 1 ($t < 0.15$ s)

In this mode, the power generation from RES (P_{RES}) is assumed as lesser than the load power (P_L). During this time, the load requirement is not met by the RES entirely. Hence, the grid supplies the lacking requirement of the load i.e. the load real power is shared by the grid real power (P_g) and inverter real power (P_c) ($P_L = P_c + P_g$). Now the grid voltage and grid current are in phase with each other. The reactive power of the load (Q_L) is fully supplied by the inverter making zero grid reactive power (Q_g) (inverter reactive power, $Q_c = Q_L$, $Q_g = 0$).

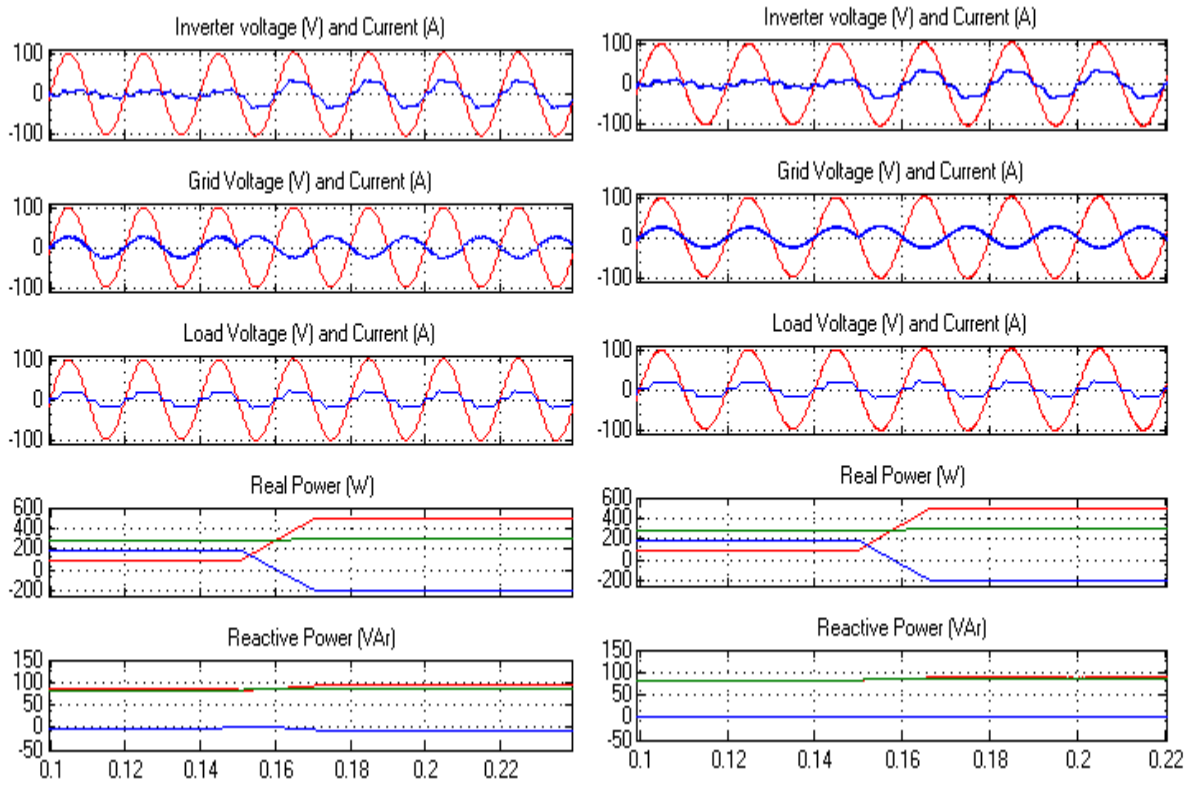

Fig. 6 Simulated results of inverter, grid, load voltage and current, (a) Hysteresis Controller, (b) LQR.

Mode 2 (t > 0.15s)

In this case, the power generation from RES (P_{RES}) is taken as greater than the load power. During this time, the load requirement is met by the RES entirely and the excess power generated by RES is fed to the grid, i.e. the inverter real power is shared by the grid real power and load real power ($P_c = P_L + P_g$). Now the grid voltage and grid current are out of phase with each other since the direction of current changes. As in mode1, the reactive power of the load is fully supplied by the inverter, making zero grid reactive power ($Q_c = Q_L$, $Q_g = 0$).

From the simulation results, it is observed that the hysteresis controller works well in mode1, but in mode 2 some reactive power is drawn from the grid. However, in both the modes, LQR relieves the grid from the reactive power. Table 2 shows the power factor and THD values for hysteresis controller and LQR. It is inferred that the power factor is nearer to unity and the THDs are lesser than IEEE limit of 5%. This shows the robustness of LQR.

Table 2

Simulated power factor and THD values for mode 1 and mode 2 operation

Factors	Hysteresis		LQR	
	Mode 1	Mode 2	Mode 1	Mode 2
Power factor	0.9964	-0.9955	0.9991	-0.9992
THD (%)	7.6	8.1	3.75	3.09

6. Experimental Results

A prototype is developed with the same specifications used in simulation to verify the control methodologies. The prototype consists of an inverter, filter, controller, autotransformer and non-linear load. The inverter is built using intelligent power module (PM25RL1A120) and connected to grid through filter inductors, grid inductors and autotransformer. The diode bridge rectifier (TSPR60PB) with resistance load is connected at PCC through rectifier link inductors. The experimental load currents (i_{La}, i_{Lb} and i_{Lc}) are shown in fig. 7. The real power, reactive power and THDs are found as 294 W, 90 var and 25.4 % respectively. The control algorithm is developed using Spartan 6 of FPGA family for the reference current generation using instantaneous p-q theory, and the controllers using hysteresis and LQR.

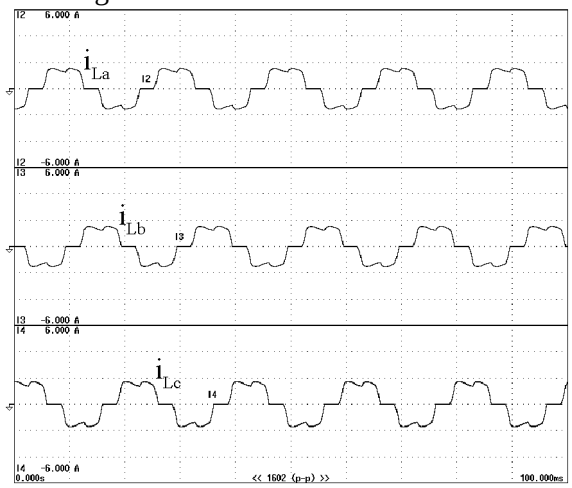

Fig. 7 Experimental Results of load currents in phases ‘a’, ‘b’ and ‘c’.

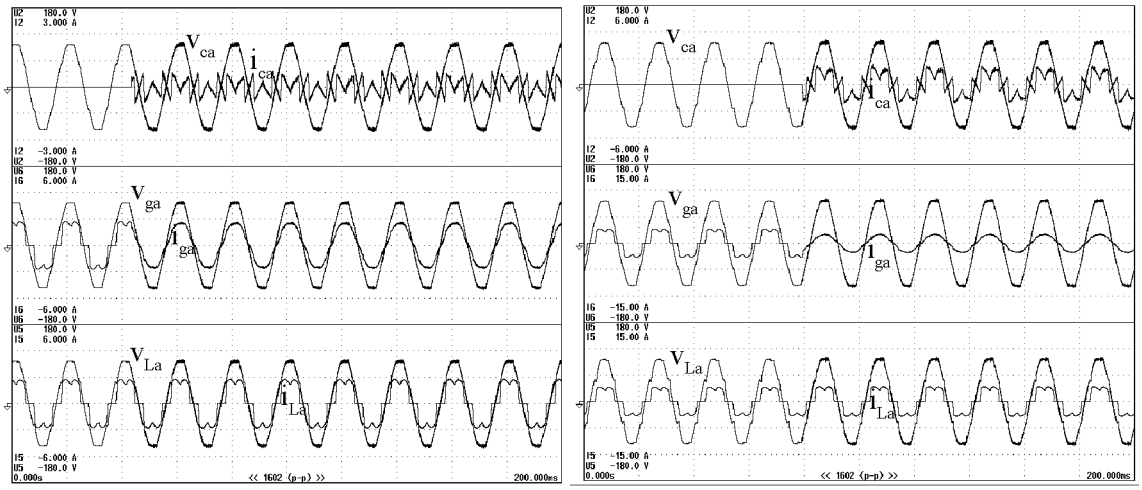

Fig. 8 Experimental Results of inverter, grid, load voltage and current in phase ‘a’ for mode 1 operation (a) Hysteresis Controller, (b) LQR.

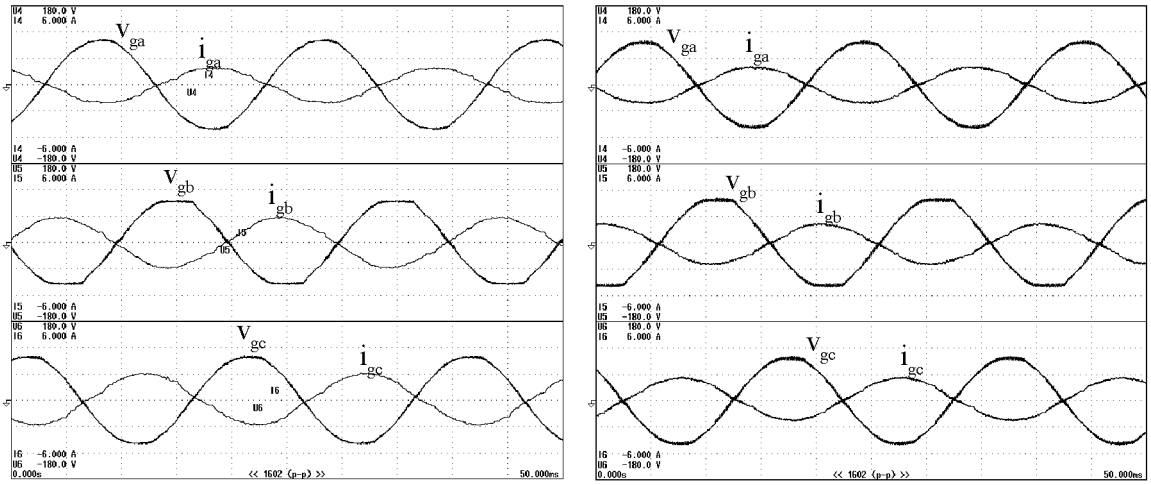

Fig. 9 Experimental results of grid voltages and currents in phases ‘a’, ’b’ and ‘c’ for mode 2 operation, (a) Hysteresis controller, (b) LQR.

To highlight the performance of LQR than the hysteresis controller, the inverter is operated in two modes which depend on the power generation from RES. Fig. 8 shows the experimental results of inverter, grid and load voltage and current for mode 1 operation controlled using hysteresis controller and LQR. At the beginning, the inverter is not connected to the system, so the grid current supplies the load. Therefore, the grid current is equal to the load current. The inverter is connected after few cycles to inject the reactive power required by the load and the real power depending on the power availability of RES. Fig. 9 shows the experimental voltages of grid voltages and currents in phases ‘a’, ‘b’ and ‘c’ for mode 2 operation. In both the modes, the inverter compensates the harmonic and reactive power components making grid current sinusoidal.

Mode 1 ($P_{RES} < P_L$)

The RES power is lower compared to load power is considered in this mode. Therefore, RES is unable to meet the load entirely. So the grid feed the remaining power required by the load. During this mode, the grid current flows towards PCC. Hence the grid voltage and current are in phase with each other. The entire reactive power of the load is compensated by the inverter. Here, P_{RES} = 39 W, P_g = 155 W, Qg = 0.

Mode 2 ($P_{RES} > P_L$)

Higher RES power than load power is assumed in this mode. The surplus power supplied by the RES is fed to the grid. Now, the grid current flows from PCC, therefore, the grid voltage and current are out of phase with each other. The load reactive power is supplied by the inverter. Here, P_{RES} = 364 W, P_g = - 210 W.

Table 3 shows the experimental values of power factor and THD for mode 1 and mode 2 operation using hysteresis controller and LQR. It is observed that LQR provides superior performance than hysteresis by giving low THD and power factor nearer to unity rather than hysteresis controller.

Table 3

Experimental power factor and THD values for mode 1 and mode 2 operation

Factors	Hysteresis		LQR	
	Mode 1	Mode 2	Mode 1	Mode 2
Power factor	0.9951	- 0.9679	0.9921	-0.9952
THD (%)	6	6.9	4.8	4.9

7. Conclusion

This paper presented the control techniques such as conventional hysteresis and linear quadratic regulator to enhance the power quality by controlling the inverter current. The CCVSI is employed to transfer the real power from RES and to compensate the reactive power by generating the reference current using instantaneous p-q theory. This theory uses instantaneous values rather than average values. But this method is unsuitable for unbalanced grid conditions. The control strategies made the grid to supply/receive sinusoidal currents with lower THD and better power factor. The LQR is designed using single phase equivalent circuit of three phase grid integrated renewable energy system thus reduces the complexity of the design. The supremacy of LQR than hysteresis controller is identified by getting low THD of less than 5% (IEEE limits) and power factor nearer to unity. Moreover, the performance is verified for two modes of operation which depends on the available power in RES. The efficacy of LQR is revealed through simulation and experimental results.

References

1. S.Y. Lin and J. F. Chen, *Distributed optimal power flow for smart grid transmission system with renewable energy sources.* Energy, 2013, 56, pp. 184 – 192.
2. A. Timbus, M. Liserre and R. Teodorescu, *Evaluation of current controllers for Distributed Power Generation Systems*, IEEE Transactions on Power Electronics, 2009, 24(3), pp. 654 – 664.
3. E.H.E. Bayoumi, *Power Electronics in Renewable Energy Smart Grid: A Review*, International Journal of Industrial Electronics and drives, 2015, 2(1), pp. 43-61.
4. E.H.E. Bayoumi, *Dual-input DC-DC Converter for Renewable Energy*, Electromotion Scientific Journal, 2014, 21(2), pp. 77-84.
5. F. Blaabjerg, R. Teodorescu, M. Liserre and A. Timbus, *Overview of Control and Grid Synchronization for Distributed Power Generation Systems*, IEEE Transactions on Industrial Electronics, 2006, 53(5), pp. 1398 – 1409.
6. X. Liang, *Emerging Power Quality Challenges Due to Integration of Renewable Energy Sources*, IEEE Transactions on Industrial Electronics, 2017, 53(2), pp. 855-866.
7. P. Schavemaker and P. V. Sluis, *Electric Power System Essentials*. West Sussex, England, John Wiley and Sons Ltd, 2008, pp. 221 – 236.
8. J.P.Pinto, R.Pregitzer, L.F.C.Monteiro and J.L. Afonso, *3-phase 4-wire shunt active power filter with renewable energy interface*, In: Proc IEEE Conf. Renewable Energy & Power Quality, Seville, Spain, 2007.
9. S.Rajendran, U.Govindarajan, A.B.Reuben and A.Srinivasan, *Shunt reactive var compensator for grid-connected induction generator in wind energy conversion systems*, IET Power Electronics, 2013, 6(9), pp. 1872 – 1883.
10. P. Garica-Gonzalez and A. Garcia-Cerrada, *Control system for a PWM-based STATCOM*, IEEE Transactions on Power Delivery, 2000, 15(4), pp. 1252–1257.
11. P. Rao, M.L.Crow and Z.Yang, *STATCOM control for power system voltage control applications*, IEEE Transactions on Power Delivery, 2000, 15(4), pp. 1311–1317.
12. A.H.Norouzi and A.M.Sharaf, *Two control schemes to enhance the dynamic performance of the STATCOM and SSSC*, IEEE Transactions on Power Delivery, 2005, 20(1), pp. 435–442.
13. M. Singh, V.Khadkikar, A.Chandra and R.K.Varma, *Grid Interconnection of Renewable Energy Sources at the distribution level with power-quality improvement features*, IEEE Transactions on Power Delivery, 2011, 26(1), pp. 307 – 315.
14. T. Zaveri and B.R.Bhalja, N. Zaveri, *A novel approach of reference current generation for power quality improvement in three-phase, three-wire distribution system using DSTATCOM*, Electrical Power and Energy Systems, 2011, 33, pp. 1702 – 1710.
15. H. Akagi, Y. Kanazawa and A. Nabae, *Generalized theory of the instantaneous reactive power in three-phase circuits*, In Proceedings of International Power Electronics Conference, Tokyo, Japan, 1983, pp. 1375–1386.
16. F. Gonzalez-Espin, E. Figueres and G. Garcera, *An adaptive synchronous-reference-frame phase-locked loop for power quality improvement in a polluted utility grid*, IEEE Transactions on Industrial Electronics, 2012, 59(6), pp. 2718–2731.
17. A. Ghosh and G. Ledwich, *Power quality enhancement using custom power devices*, 1st Edition, Kluwer Academic Publishers, 2002, pp. 241 – 286.
18. H.Agaki, E.H. Wantanabe and M. Aredes, *Instantaneous power theory and applications to power conditioning*, IEEE Press, NJ, John Wiley and Sons Ltd, 2007, pp. 19 – 40.

19. T. Hornik, and Q. Zhong,, *A Current-Control Strategy for Voltage-Source Inverters in Microgrids Based on H∞ and Repetitive Control*, IEEE Transactions on Power Electronics, 2011, 26, pp. 943 – 952.
20. K. Ogata, *Modern Control Engineering*. 5th edition, Prentice Hall, 2010.
21. R. Vinifa and A. Kavitha, *Linear Quadratic Regulator Based Current Control of Grid Connected Inverter for Renewable Energy Applications*, In : Proc of IEEE Conf Energy Efficient Technologies for Sustainability, Nagercoil, India, 2016.